

Controlling multivalent binding through surface chemistry: model study on streptavidin

Galina V. Dubacheva^{†‡*}, Carolina Araya-Callis[†], Anne Geert Volbeda^{||}, Michael Fairhead[⊥],
Jeroen Codée^{||}, Mark Howarth[⊥] and Ralf P. Richter^{†§#*}

[†]Biosurfaces Lab, CIC biomaGUNE, Paseo Miramon 182, 20014 Donostia - San Sebastian, Spain

[‡] PPSM CNRS, ENS Cachan, Université Paris-Saclay, 61 Avenue du Président Wilson, 94235 Cachan, France

[⊥]Department of Biochemistry, University of Oxford, Oxford, OX1 3QU, United Kingdom

^{||}Leiden Institute of Chemistry, Leiden University, P.O. Box 9502, 2300 RA Leiden, The Netherlands

[§] School of Biomedical Sciences and School of Physics and Astronomy, University of Leeds, Leeds, LS2 9JT,
United Kingdom

[#]Laboratory of Interdisciplinary Physics, University Grenoble Alpes - CNRS, 140 Rue de la Physique, 38402 Saint
Martin d'Hères, France

Supporting information

SUPPORTING METHODS

Synthesis, purification and characterization of b-oHA. The b-oHA oligomer was assembled by functionalization of an HA pentadecasaccharide generated by automated solid phase synthesis.¹ The modification was performed in two steps through a thiol-ene reaction with cysteamine followed by a condensation with biotin-OSu. First, 2.25 mg of hyaluronic acid pentadecasaccharide (0.77 μmol) was added to 1.4 mL degassed H_2O containing 0.88 mg (7.7 μmol , 10 eq) cysteamine·HCl. The solution was transferred to a glass tube under an argon atmosphere, and irradiated with a UV lamp (4 W, $\lambda = 254$ nm). After ~ 3 h, the solvent was removed under reduced pressure. The compound was purified by HW40 size-exclusion chromatography (eluted with NH_4OAc) and lyophilized to give the cysteamine functionalized oligosaccharide (2.22 mg, 0.71 μmol , 92%; **1** in Fig. S1A). Second, the functionalized pentadecasaccharide **1** (2.22 mg, 0.71 μmol) was dissolved in 50 μL H_2O . Then 50 μL 0.057 M Biotin-OSu in DMF/ Et_3N 9:1 was added to the solution, the mixture was allowed to shake for 4 h 20 min, and the concentrated solution was collected. Purification by HPLC (Fig. S1B) yielded the biotin functionalized pentadecasaccharide (0.88 mg, 0.27 μmol , 39%; **2** in Fig. S1A). HRMS: $[\text{M}+2\text{H}]^+ m/z$ 2, calcd for $\text{C}_{121}\text{H}_{187}\text{N}_{11}\text{O}_{85}\text{S}_2$ 1610.51336, found 1610.51541.

^1H NMR (600 MHz, D_2O , Fig. S1C) δ 4.67 – 4.39 (m, 17H), 4.00 – 3.90 (m, 11H), 3.88 – 3.85 (m, 4H), 3.85 – 3.81 (m, 5H), 3.78 – 3.67 (m, 29H), 3.63 – 3.57 (m, 8H), 3.57 – 3.45 (m, 20H), 3.42 (t, $J = 6.5$ Hz, 2H, biotin-spacer), 3.40 – 3.33 (m, 9H), 3.01 (dd, $J = 13.1, 5.0$ Hz, 1H, biotin-spacer), 2.80 (d, $J = 13.1$ Hz, 1H, biotin-spacer), 2.75 – 2.69 (m, 2H, biotin-spacer), 2.66 – 2.57 (m, 2H, biotin-spacer), 2.29 (t, $J = 7.3$ Hz, 2H, biotin-spacer), 2.06 (s, 3H, CH_3 NHAc), 2.06 – 2.02 (m, 21H, 7 x CH_3 NHAc), 1.90 – 1.81 (m, 2H, biotin-spacer), 1.79 – 1.70 (m, 2H, biotin-spacer), 1.70 – 1.56 (m, 4H, biotin-spacer), 1.49 – 1.40 (m, 2H, biotin-spacer).

Expression, purification and characterization of b-ZZ. The b-ZZ protein (16.2 kDa) was expressed from the pCA1 plasmid encoding a precursor protein with a polyhistidine (H_{14}) tag at the N-terminus followed by a *B. distachyon* small ubiquitin-like modifier (bdSUMO) protease² cleavage recognition sequence, an Avi-tag sequence for BirA biotin ligation, and a repeat of the IgG-binding Z-domain of protein A. The amino acid sequence of the final protein including spacers is given in Fig. S2A, and the complete pCA1 plasmid sequence is available on request.

To produce b-ZZ, the pCA1 plasmid and a BirA encoding plasmid (pSF2174, kindly provided by Steffen Frey, Max Planck Institute for Biophysical Chemistry, Göttingen, Germany) were co-transformed in NEB Express *E. coli* (New England Biolabs, Cat. No. C2523). The cells were grown in TB medium supplemented with 50 $\mu\text{g}/\text{mL}$ kanamycin and 50 $\mu\text{g}/\text{mL}$ spectinomycin at 37°C. At $\text{OD}_{600} = 0.4$, the culture was induced with 0.25 mM IPTG, 20 $\mu\text{g}/\text{mL}$ biotin were added and the temperature was reduced to 20°C. After overnight incubation, 5 mM of EDTA were added to the culture. Cells were harvested by centrifugation and the cell pellet was re-suspended in buffer made of 44 mM Tris-HCl (pH 7.5), 290 mM NaCl, 4.4 mM MgCl_2 , 15 mM imidazole, and 10 mM DTT. Cells were disrupted by sonication and the lysate was cleared by centrifugation at 40000 g and 4°C for 1 h. Cleared lysate was added to a pre-equilibrated cComplete His-Tag Purification Resin (Roche, Cat. No. 05893682001) and incubated at 4°C at gentle shaking for 1 hr. After 5 washing steps, the resin was transferred to a column. For cleavage of the H_{14} tag from the precursor protein, one column volume of the Tris-HCl buffer containing 100 nM bdSUMO protease² was added to the resin and incubation was performed overnight at 4°C. One column volume of Tris-HCl buffer was added to recover the cleaved protein. Cut proteins were further purified by gel filtration on a Superdex200 16/60 column (GE Healthcare)

pre-equilibrated with Tris-HCl buffer containing 5 mM DTT. The purified protein was diluted to a concentration of 6 mg/mL, supplemented with sucrose (250 mM final concentration), and frozen in liquid nitrogen for storage.

SDS-PAGE analysis (Fig. S2B) confirmed the correct molecular weight and purity of b-ZZ. Successful biotinylation was confirmed by QCM-D monitoring of specific b-ZZ binding to rSAV-coated b-SLBs and b-SAMs (Figs. 5 and S3B, D).

SUPPORTING FIGURES

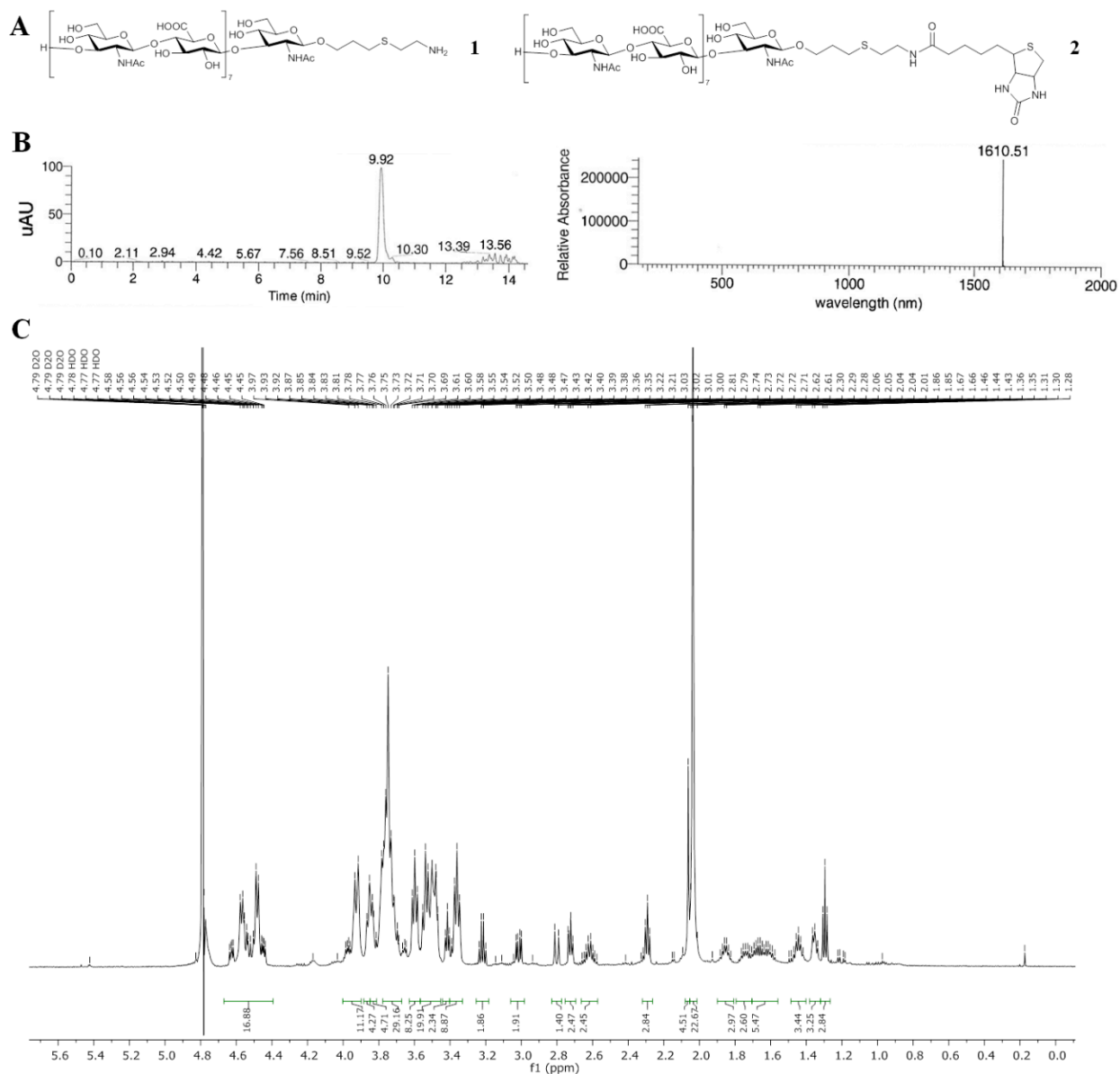


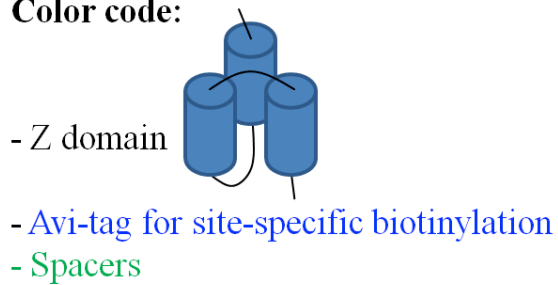
Figure S1. Chemical structure and characterization of b-oHA. (A) Chemical structures of cystamine-functionalized oHA (**1**) and b-oHA (**2**). (B) HPLC profile (*NOMURA* chemical Develosil RPAQUEOUS column, 5 → 17% acetonitrile in 0.1% TFA in H₂O; Agilent 1200 Series, Agilent 6130 Quadruple MS detector) and HRMS (Thermo Finnigan LTQ Orbitrap) of b-oHA. (C) ¹H NMR (600 MHz, D₂O; Bruker DMX-600 (600/150 MHz) spectrometer) of b-oHA.

A

b-ZZ sequence:

AGTGGLNDIFEAQKIEWHEGSGSAGSTPGSSN
KFNKEQQNAFYEILHLPNLNEEQRNGFIQSLK
DDPSQSANLLAEAKKLNDAQAPKGSNKFNKE
QQNAFYEILHLPNLNEEQRNGFIQSLKDDPSQ
SANLLAEAKKLNDAQAPK

Color code:



B

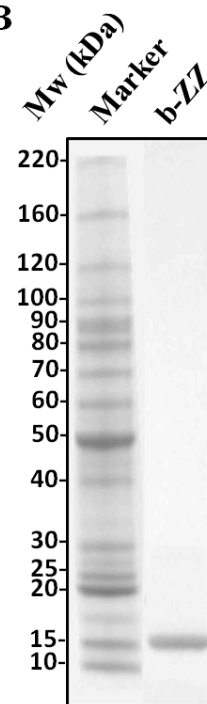


Figure S2. Primary structure and characterization of b-ZZ. (A) Amino acid sequence (single letter code) of b-ZZ including two concatenated Z domains of protein A (black), and an Avi-tag (blue). (B) SDS-PAGE characterization of purified b-ZZ, showing a single band close to the molecular mass of 16.2 kDa calculated for the biotinylated sequence after Coomassie staining.

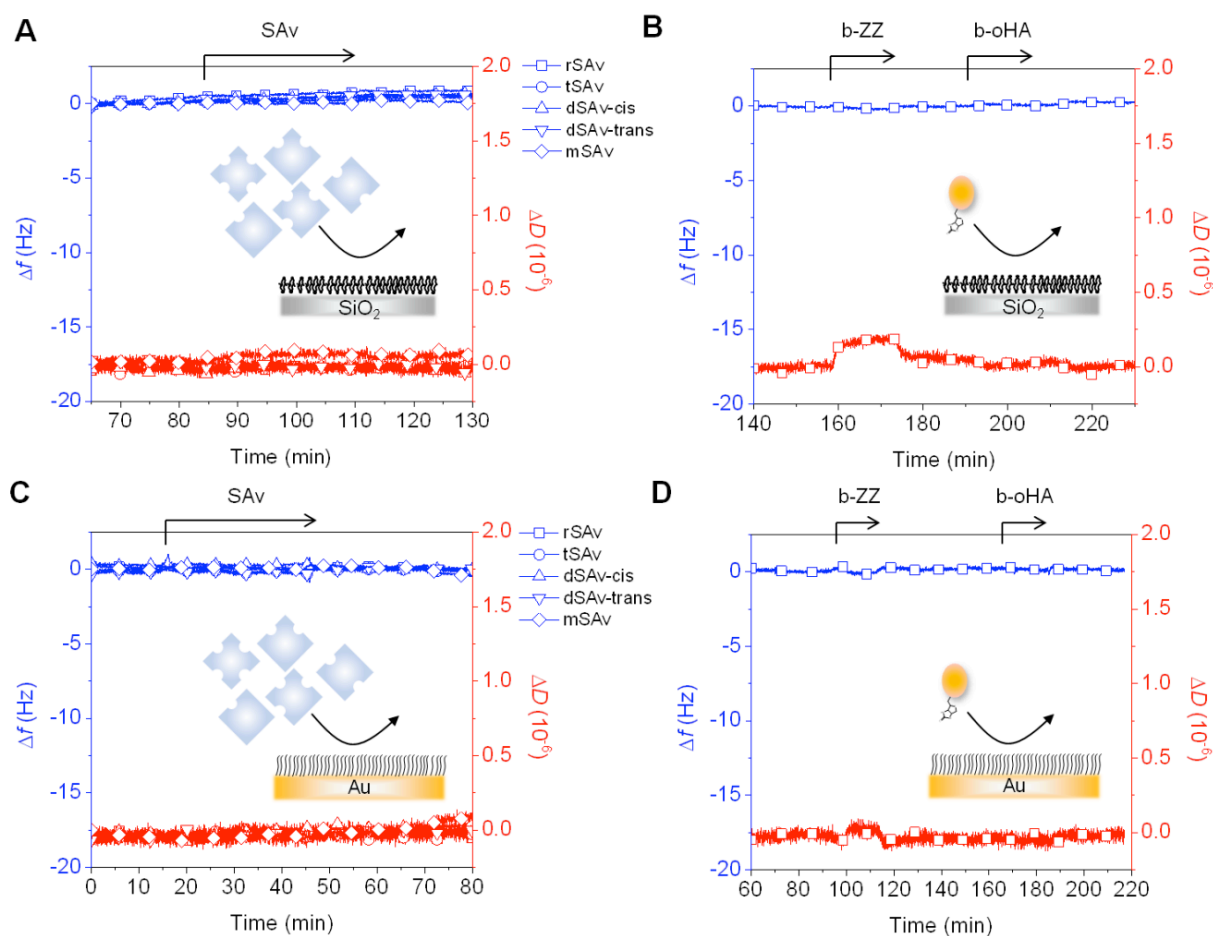


Figure S3. Specificity of adsorption to SLBs and SAMs. QCM-D shows no shifts in f and D upon interaction of rSAV, tSAV, dSAV-cis, dSAV-trans and mSAV (A, C) and the biotinylated probes b-ZZ and b-oHA (B, D) with b0%-SLBs (made of pure DOPC; A, B) and b0%-SAM (made of pure HS-(CH₂)₁₁-EG₄-OH; C, D). These results indicate that the binding events in this study are specific, i.e. they are entirely due to SAV/biotin interactions. Insets: schematic representations of the interfaces and interactions probed. Conditions: SAV adsorption time – 30 min, biotinylated probe adsorption time – 15 min, $c_{\text{SAV}} = 10 \mu\text{g/mL}$, $c_{\text{b-ZZ}} = 36 \mu\text{g/mL}$, $c_{\text{b-oHA}} = 5 \mu\text{g/mL}$, flow rate – 20 $\mu\text{L/min}$.

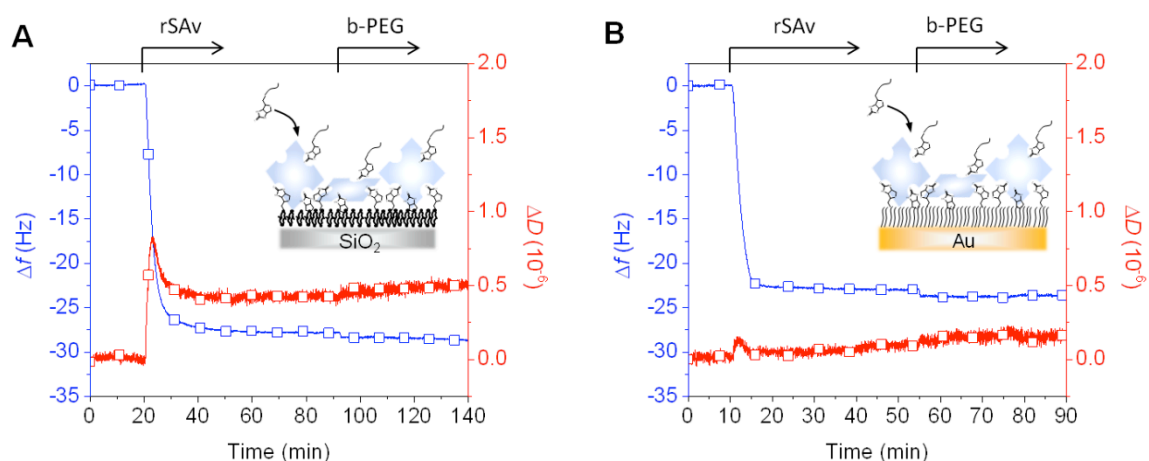


Figure S4. SAV cannot be eluted by biotinylated probes in the solution phase. The QCM-D responses upon formation of rSAv monolayers on b5%-SLB (A) and b10%-SAM (B) and their subsequent exposure to b-oEG are shown. b-oEG (Sigma-Aldrich) is made of 9 EG units (contour length 3.5 nm) and a terminal biotin, and was selected for competition experiments because its small size and flexibility provide for easy access to binding sites. The small negative shifts in f upon b-oEG incubation indicate binding. No increase in f is observed, demonstrating that SAV detachment does not occur. Insets: schematic representations of the interfaces and interactions probed. Conditions: SAV adsorption time – 30 min, $c_{\text{SAV}} = 10 \mu\text{g/mL}$, b-oEG adsorption time – 20-30 min, $c_{\text{b-oEG}} = 20 \mu\text{g/mL}$, flow rate – $20 \mu\text{L/min}$.

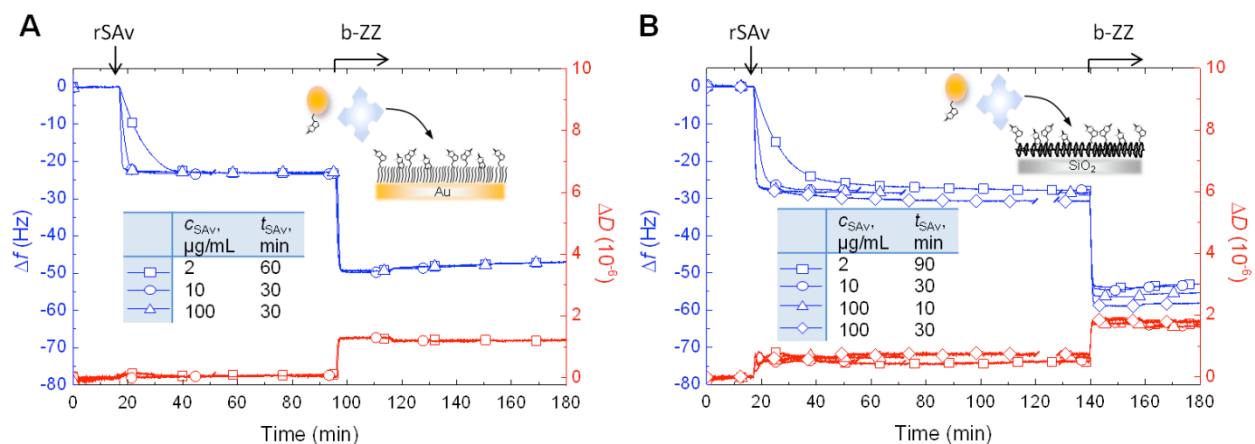


Figure S5. The SA_v concentration does not affect the surface density and presentation of SA_v at saturation by biotinylated surfaces. QCM-D responses obtained for the binding of rSA_v and subsequently b-ZZ to b10%-SAMs (A) and b5%-SLBs (B) as a function of SA_v concentration (c_{SAv}) and exposure time (t_{SAv}) as indicated in the table insets. As expected, the initial rSA_v binding rate increases with rSA_v concentration. However, the final SA_v coverage (which is close to a saturated monolayer) and residual valency (probed through the binding of b-ZZ) are not substantially affected by the rSA_v concentration. Insets: schematic representations of the interfaces and interactions probed. Conditions: b-ZZ adsorption time – 15 min, $c_{b-ZZ} = 36 \mu\text{g/mL}$.

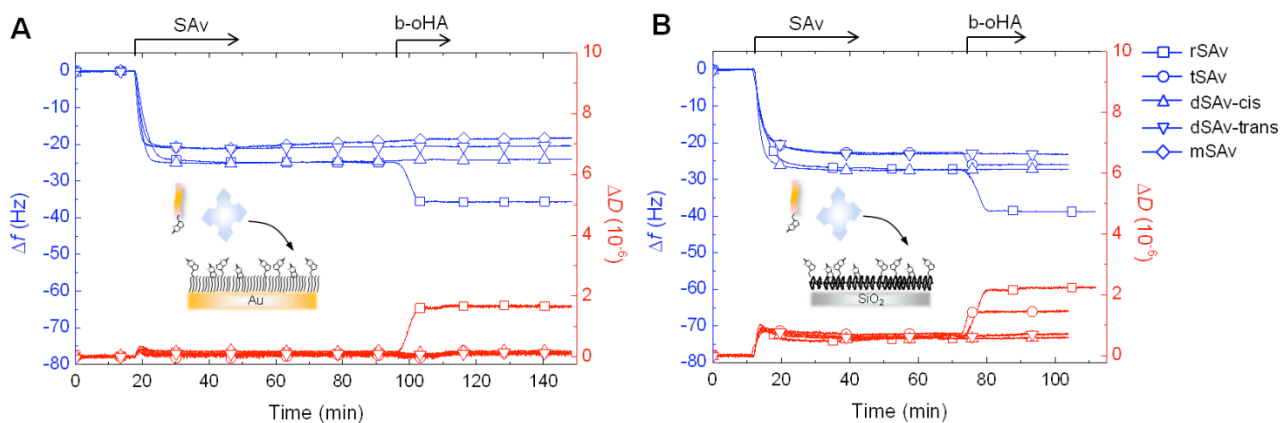


Figure S6. Binding assays with b-oHA reproduce the results with b-ZZ. Typical QCM-D responses obtained for the binding of SAV, and subsequently b-oHA, to b10%-SAM (A) and b5%-SLB (B). SAV constructs: rSAV (squares), tSAV (circles), dSAV-cis (upward-pointing triangles), dSAV-trans (downward-pointing triangles) and mSAV (lozenges). The responses are qualitatively fully consistent with the analogous measurements using b-ZZ instead of b-oHA shown in Fig. 4. Conditions: SAV adsorption time – 30 min, biotinylated probe adsorption time – 15 min, $c_{\text{SAV}} = 10 \mu\text{g/mL}$, $c_{\text{b-oHA}} = 5 \mu\text{g/mL}$.

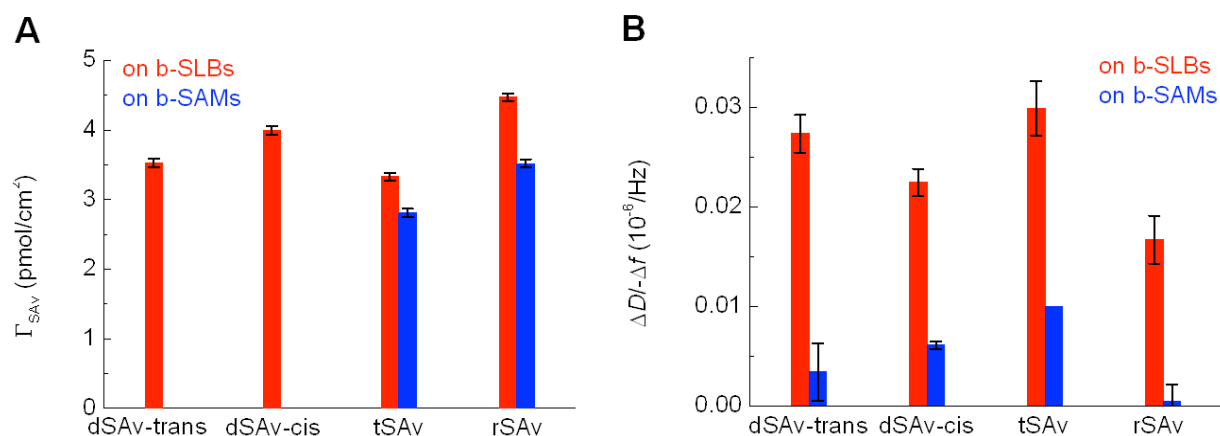
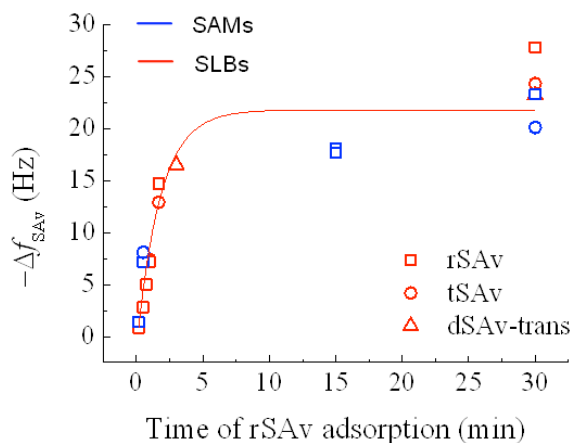


Figure S7. SLBs and SAMs offer binding interfaces with distinct surface densities and mechanical properties. (A) Surface densities of SAves, Γ_{SAV} , were determined by SE after 90 min adsorption at 10 $\mu\text{g/mL}$ and extensive buffer rinsing (Fig. 6, Table S1). The data show that denser monolayers are formed on SLBs (compared to SAMs), and for cis-oriented (compared to trans-oriented) constructs. (B) Ratios of $\Delta D/\Delta f$ were extracted for SAves binding at saturation (representative data are shown in Figs. 5 and S6) and are a measure of the mechanical compliance of the interface between SAves and the biotinylated surface. Error bars represent standard deviations. The interface is consistently softer for SLBs than for SAMs.

A Tuning SAv adsorption time



B Tuning biotin density

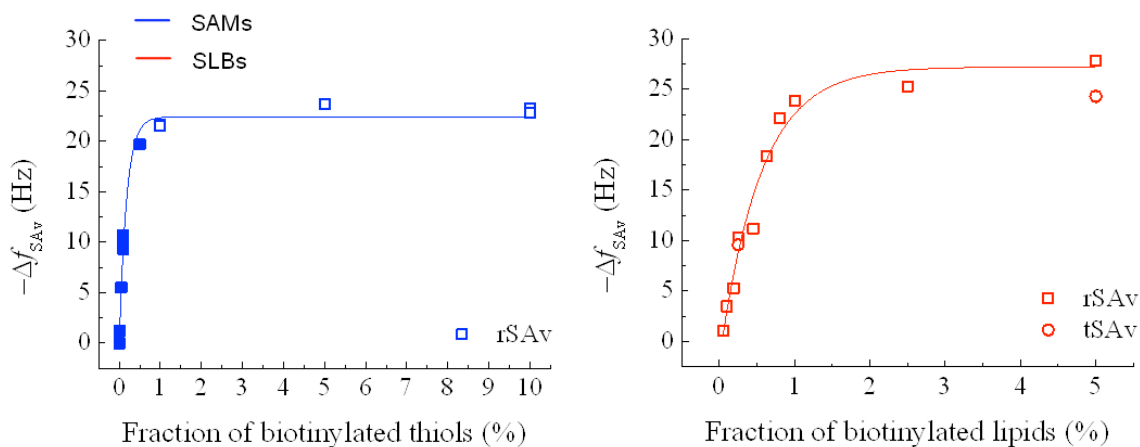


Figure S8. Dependence of SAv coverage on SAv adsorption time and biotin surface content.

(A) The SAv adsorption time was varied from 10 s to 30 min at fixed biotin surface densities (b10%-SAM - blue, b5%-SLB - red). (B) The biotin surface density was varied (from 0 to 10% for b-SAMs - blue, from 0 to 5% for b-SLBs - red) at fixed SAv adsorption time (30 min). Both sets of measurements were performed at $c_{SAV} = 10 \mu\text{g/mL}$. $-\Delta f$ were collected at saturation (representative data are shown in Figs. 5, 8, S6 and S9) and reflect the resulting mass uptakes for rSAv (squares), tSAv (circles) and dSAv-trans (triangles). The filled data points correspond to the range where SAv binding was not stable (due to the lack of multivalent attachment) and were collected after an extensive (1-2 h) buffer rinsing, when signals had reached a quasi-plateau. Lines are guides for the eyes. The obtained trends are consistent with the analogous measurements by SE (Table S1).

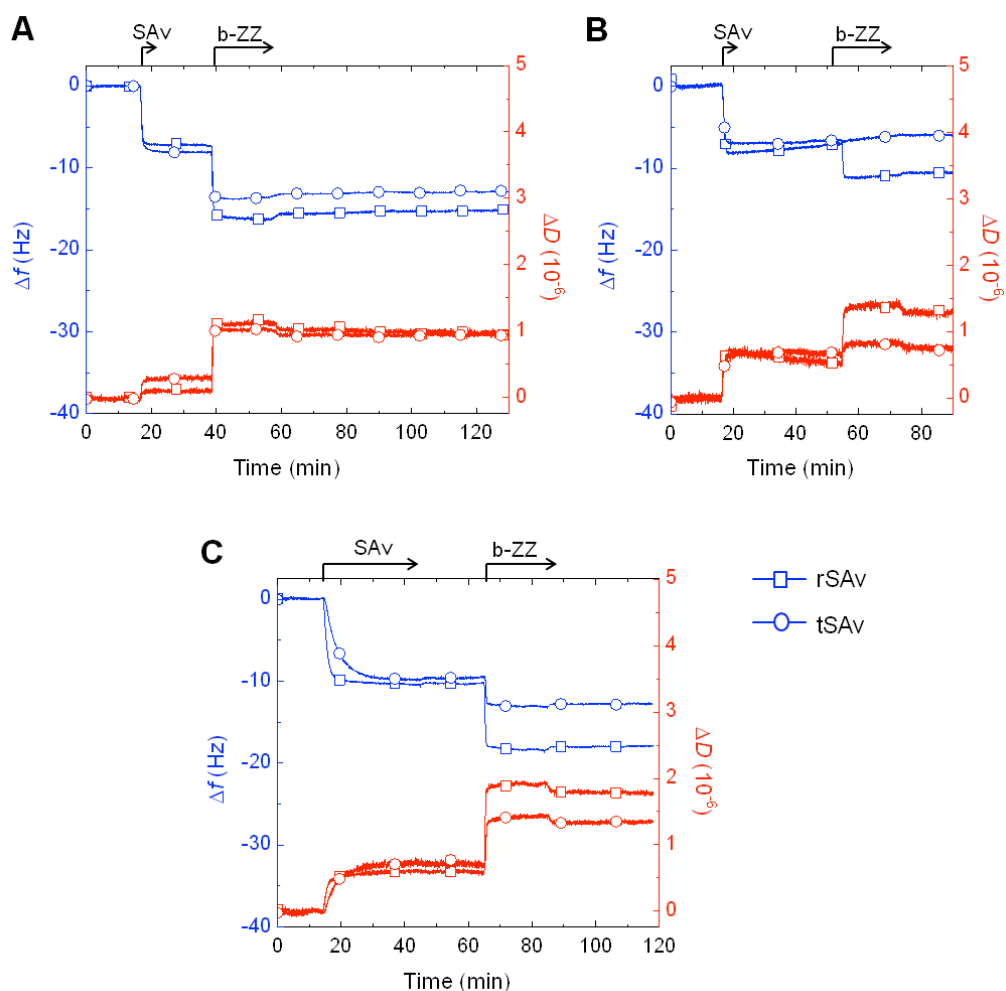


Figure S9. Representative QCM-D data at sub-monolayer SAV coverages. Typical QCM-D responses are obtained during the binding of SAV, and subsequently b-ZZ, to (A) b5%-SAM and (B) b5%-SLB with SAV binding controlled by incubation time and (C) b0.3%-SLB with SAV incubated to saturation. SAV constructs: rSAV (squares), tSAV (circles). Conditions: SAV adsorption time – 30 s (A), 60 s (B) or 30 min (C), b-ZZ adsorption time – 20 min, $c_{\text{SAV}} = 10 \mu\text{g/mL}$, $c_{\text{b-ZZ}} = 36 \mu\text{g/mL}$.

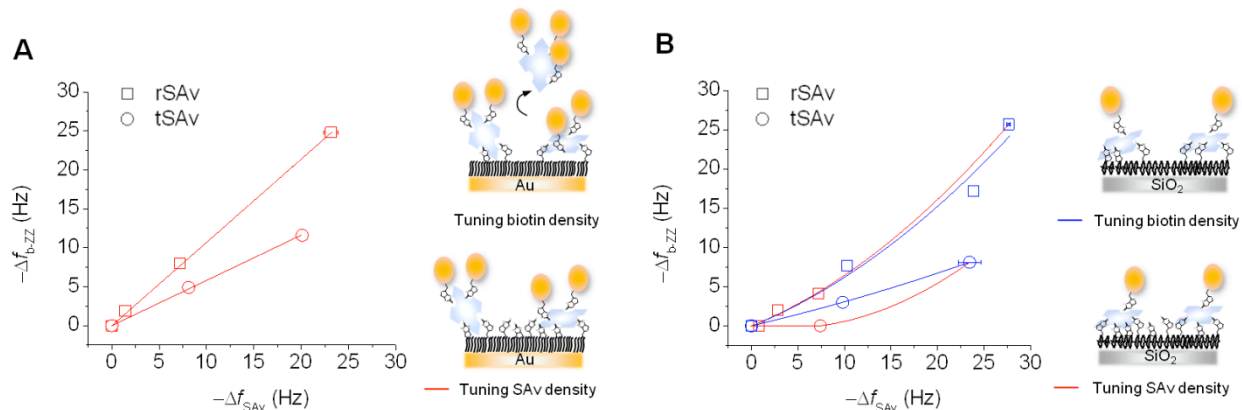


Figure S10. Complementary QCM-D data for the effect of SAV coverage and biotin surface density on SAV (rSAV and tSAV) interactions with biotinylated surfaces. (A) Surfaces with immobile biotin. $-\Delta f_{b-ZZ}$ plotted vs. $-\Delta f_{SAV}$ for SAV binding to b-SAM together with schematic representations of SAV films at low biotin surface density (top) and low SAV coverage (bottom). The plots correspond to the case when the adsorption time of SAV binding to b10%-SAM is varied from 30 s to 30 min; the data at different biotin surface densities are not shown because SAV binding at low biotin surface densities was not stable (Fig. 8A). (B) Surfaces with laterally mobile biotin. $-\Delta f_{b-ZZ}$ plotted vs. $-\Delta f_{SAV}$ for SAV binding to b-SLB together with schematic representations of SAV films at low biotin surface density (top) and low SAV coverage (bottom). In one case, biotin surface density was varied between 0 and 5% at SAV adsorption time fixed to 30 min (blue). In the other case, the adsorption time of SAV binding is varied from 30 s to 30 min at fixed biotin surface density (b5%-SLB; red). The plotted Δf_{b-ZZ} and Δf_{SAV} were recorded after binding and buffer rinsing, once the QCM-D response had stabilized; representative QCM-D binding curves are shown in Figs. 5 and S9. Lines are linear or parabolic fits. Conditions: b-ZZ adsorption time – 20 min, $c_{SAV} = 10 \mu\text{g/mL}$, $c_{b-ZZ} = 36 \mu\text{g/mL}$.

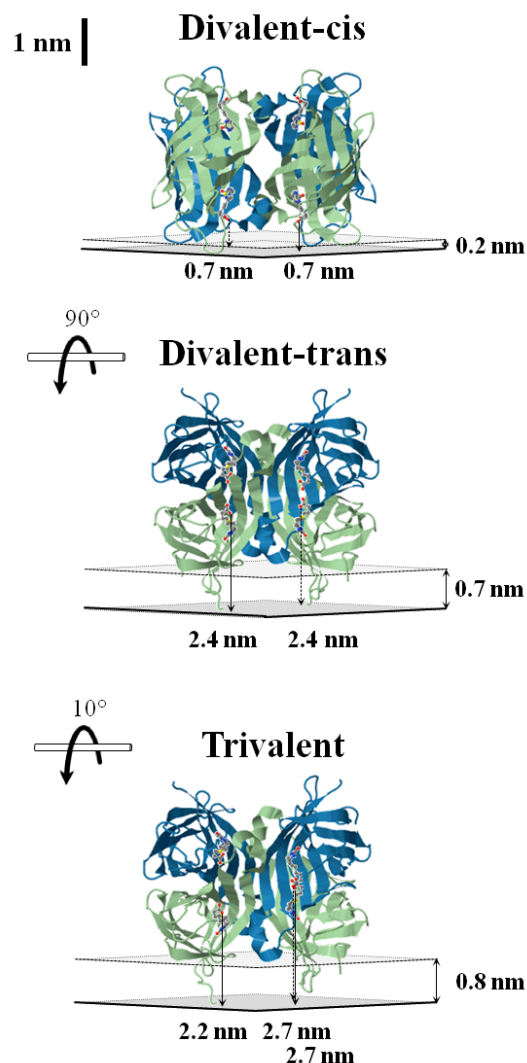


Fig. S11. Orientation of surface-bound SAv. SAv tetramers (PDB entry 3ry2) are shown in a ribbon representation with two monomers in blue and two monomers in green color. 4 biotins are superposed in front as ball-and-stick diagrams at horizontal and vertical positions according to their respective binding pockets in the SAv. SAv orientations are chosen such that the distances of the biotins' -COOH groups (O atoms: O11 #2012 and #4391 in cis; O11 #2040 and #4391 in trans, O11 #2040, #4391 and O12 #4364 in trivalent) from the surface plane (shown in gray; black arrows pointing to the surface plane indicate these distances and also the relative position of the biotins in the third dimension) are minimized for two biotins arranged in cis, for two biotins arranged in trans, and for three biotins. Rotations required to move between these orientations are also indicated (horizontal lines and circular arrows represent the rotation axes and directions, respectively). The estimated distances to the surface plane are 0.7 nm for divalent binding in cis, 2.4 nm for divalent binding in trans, and between 2.2 and 2.7 nm for trivalent binding. We note that these distances are obtained assuming complete exclusion of the SAv from the surface. In reality, surface-proximal loops of SAv may be deformed or embedded in the self-assembled monolayer or in the supported lipid bilayer, reducing the effective distances. This is illustrated by a second surface plane (shown transparent with dotted front borders) the position of which was chosen such that flexible loops but not the presumably more rigid beta sheet forming body of the protein can 'mold' into the surface. This reduces the distances by between 0.2 and 0.8 nm depending on the orientation. We propose that embedding/deformation of streptavidin peripheral loops, out-of-plane movement of lipids and stretching of flexible linkers connecting the biotins to the SAM and SLBs all contribute to enable the binding of biotins into their binding pockets in SAv. Structural models were prepared and distances estimated in JSmol.

Table S1. Quantification of the mean SA_v residual valency. SA_v valency, biotin surface density and lateral mobility, and SA_v surface density (Γ_{SA_v}) were tuned; the effects on the surface density of biotinylated probes (Γ_b) and on the mean SA_v residual valency (equivalent to the ratio Γ_b/Γ_{SA_v}) were quantified by SE. Conditions (unless otherwise stated): $c_{SA_v} = 10 \mu\text{g/mL}$, $c_{b-ZZ} = 36 \mu\text{g/mL}$, $c_{b-oHA} = 5 \mu\text{g/mL}$; Γ_{SA_v} and Γ_b were determined after adsorption and buffer rinsing until stabilization of the SE response.

SA _v construct	Surface	SA _v		Biotinylated probe		Γ_b/Γ_{SA_v}
		Adsorption time	Γ_{SA_v} , pmol/cm ²	Construct	Γ_b , pmol/cm ²	
rSA _v	b10%-SAM	90 min	3.52	b-oHA	5.90	1.68
		30 min	3.45 ± 0.12 (<i>n</i> = 4)	b-ZZ	6.17	1.80 ± 0.04 (<i>n</i> = 4)
				b-ZZ	6.23	
	b-oHA			5.90		
	b-oHA			6.21		
			<i>mean ± SD</i>		6.13 ± 0.15	
	10 sec	2.22	b-ZZ	3.83	1.73	
	b1%-SAM	90 min	2.75	b-ZZ	5.37	1.95
	b5%-SLB	90 min	4.47	b-oHA	7.76	1.74
		5 min	3.83	b-oHA	6.21	1.62
		30 sec	2.38	b-oHA	3.42	1.43
		10 sec	1.63	b-ZZ	1.91	1.17
5 min*		0.83	b-oHA	0.93	1.12	
b0.625%-SLB	30 min	1.77 ± 0.05 (<i>n</i> = 2)	b-ZZ b-oHA <i>mean ± SD</i>	2.47 2.80 2.64 ± 0.16	1.50 ± 0.06 (<i>n</i> = 2)	
b0.45%-SLB	30 min	0.90	b-ZZ	1.17	1.30	
tSA _v	b10%-SAM	90 min	2.74	b-ZZ	1.79	0.65
	b1%-SAM	90 min	2.27	b-ZZ	1.98	0.87
	b5%-SLB	180 min	3.29	b-ZZ	1.23	0.37
		90 min	3.24 ± 0.05 (<i>n</i> = 3)	b-ZZ	1.30	0.42 ± 0.05 (<i>n</i> = 3)
				b-oHA	1.24	
		<i>mean ± SD</i>		1.36 ± 0.16		
1 min	1.59 ± 0.04 (<i>n</i> = 2)	b-ZZ b-oHA <i>mean ± SD</i>	0.12 0.31 0.22 ± 0.10	0.14 ± 0.07 (<i>n</i> = 2)		
dSA _v -cis	b5%-SLB	90 min	3.99	b-ZZ	0**	-
dSA _v -trans	b5%-SLB	90 min	3.53	b-ZZ	0**	-
mSA _v	b10%-SAM	90 min	3.15***	b-ZZ	-	-

* 5-times diluted SA_v solution was injected.

** Determined Γ values were below the sensitivity limit of SE (1 ng/cm²).

*** Binding was not stable; the displayed value corresponds to equilibrium binding before buffer rinsing.

SUPPORTING REFERENCES

1. Walvoort, M. T. C.; Volbeda, A. G.; Reintjes, N.; van den Elst, H.; Plante, O. J.; Overkleeft, H. S.; van der Marel, G. A.; Codée, J. D. C. *Org. Lett.* **2012**, *14*, 3776.
2. Frey, S.; Görlich, D. *J Chromatogr. A* **2014**, *1337*, 95.